Reac Kinet Mech Cat (2017) 122:229–245
DOI 10.1007/s11144-017-1217-8

Synthesis of dihydropyrano[2,3-c]pyrazoles using $Ca_{9.5}Mg_{0.5}(PO_4)_{5.5}(SiO_4)_{0.5}F_{1.5}$ as a new nano cooperative catalyst

Leila Khazdooz[1] · Amin Zarei[2] · Tahmineh Ahmadi[3] · Hamidreza Aghaei[3] · Nasrin Nazempour[3] · Laleh Golestanifar[3] · Nafisehsadat Sheikhan[4]

Received: 10 April 2017 / Accepted: 22 June 2017 / Published online: 27 June 2017

Abstract $Ca_{9.5}Mg_{0.5}(PO_4)_{5.5}(SiO_4)_{0.5}F_{1.5}$ was used as a nano cooperative catalyst for the synthesis of dihydropyrano[2,3-c]pyrazoles derivatives via a one-pot four component reaction of aldehyde, ethyl acetoacetate, malononitrile and hydrazine hydrate. The reactions were carried out at 70 °C under mild and heterogeneous conditions. The catalyst was easily synthesized by high energy ball milling and the effect of some parameters such as specific surface area, pore volume, particle size, pH and crystallinity degree of the catalyst was studied on the yield and reaction time. The used catalyst showed both Brønsted base and Lewis acid properties. The acidic sites were determined by FT-IR spectroscopy of pyridine adsorption technique at different temperature. Using a new cooperative catalyst and an environmentally benign procedure, good to high yield of the products and relatively short reaction time were the advantages of the present method.

Electronic supplementary material The online version of this article (doi:10.1007/s11144-017-1217-8) contains supplementary material, which is available to authorized users.

✉ Leila Khazdooz
Leila_khazdooz@yahoo.com

[1] Department of Science, Khorasgan (Isfahan) Branch, Islamic Azad University, Isfahan 81595-158, Iran

[2] Department of Science, Fasa Branch, Islamic Azad University, PO Box No. 364, Fasa, Fars 7461713591, Iran

[3] Department of Chemistry, Shahreza Branch, Islamic Azad University, Shahreza, Isfahan 311-86145, Iran

[4] Department of Chemistry, Faculty of Sciences, Najafabad Branch, Islamic Azad University, PO Box No. 517, Najafabad, Isfahan 8514143131, Iran

Keywords Cooperative catalyst · Apatite derivatives · Brønsted base · Lewis acid · Dihydropyrano[2,3-c]pyrazoles

Introduction

Although mono-functional catalysts are used for many types of chemical transformations, a large number of them are not proficient enough especially for the multiple-step reactions in terms of various fundamental aspects such as catalytic activity, substrate scope, selectivity and cost efficiency [1]. One of the most important routes to overcome these limitations is the use of cooperative catalysts that is the encouraging strategy to increase the reactivity and selectivity in chemical transformations [2]. It should be mentioned that unlike the traditional mono-functional catalysts, cooperative catalysts act as two or even more functional groups existing in a catalytic system, which simultaneously work to accelerate and control a chemical reaction at the same time. Among the bifunctional catalytic materials, the catalysts including the Lewis acid and the Brønsted base sites are the most important cooperative catalysts used in advanced organic and biosyntheses [2]. These types of Lewis acid-Brønsted base catalysts are commonly synthesized by using a transition metal cation coordinated with some appropriate organic ligands [2]. In these structures, the transition metal cations act as the Lewis acid and the lone pair electrons of the corresponding ligands act as the Brønsted base. These catalysts have good selectivity and reactivity in various organic reactions. However, most of them are introduced as the homogenous catalysts that can restrict their applications especially in industry. Moreover, because of using organic ligands in the structure of these catalysts, they have low thermostability. It should be mentioned that most of the organic ligands used for the synthesis of these bifunctional catalytic materials are expensive. Moreover, the preparation of these kinds of cooperative catalysts is time-consuming [2]. Therefore, the synthesis of new heterogeneous cooperative catalyst with an easy and inexpensive procedure can be desired in this area of research.

Hydroxyapatite ($Ca_{10}(PO_4)_6(OH)_2$, HA) is widely used for biomedical applications because of its biocompatible, bioactive and osteoconductive properties [3–5]. However, the applications of synthetic HA as a catalyst, are limited due to its low thermostability, high solubility, poor mechanical properties and sensitivity in acidic conditions [6–8]. One of the important methods to enhance the desirable properties of HA is the addition of special elements to the structure of hydroxyapatite by ionic substitutions [9, 10]. Mg, F and Si are the most important elements for this purpose. Fluorine-substituted HA ($Ca_{10}(PO_4)_6(OH)_{2-x}F_x$, FHA) and fluorapatite ($Ca_{10}(PO_4)_6F_2$, FA) are formed by substitution of F^- instead of OH^- [11–13]. By incorporation of fluoride to HA, the solubility decreases but thermal and chemical stability increase [11, 12]. Magnesium can be substituted instead of calcium in the structure of HA to form MgHA ($Ca_{10-x}Mg_x(PO_4)_6(OH)_2$) [14, 15]. By substitution of Mg in the hydroxyapatite structure, the porosity of this bioceramic increases [16–19]. Si-substitution hydroxyapatite ($Ca_{10}(PO_4)_{6-x}(SiO_4)_x(OH)_{2-x}$, SiHA) can be synthesized by substitution of silicate instead of phosphate ions in the structure of

HA [20–22]. It is notable that by incorporation of Si to HA, the mechanical properties and the surface area of hydroxyapatite improve [20, 23]. Recently, by simultaneously incorporation of F, Mg and Si into HA structure (Si–Mg-FA), the great biological, mechanical, physical and chemical properties have been observed [24]. Hydrothermal synthesis, hydrolysis, precipitation method, mechanochemical activation and sol–gel technique are the common methods for the preparation of synthetic hydroxyapatite derivatives [11, 23, 25, 26]. Among these systems, mechanochemical activation by high energy ball milling is one of the most effective, convenient and economical methods for the synthesis of these advanced materials [24].

Pyrano[2,3-c]pyrazoles are one of the most important class of fused heterocyclic compounds that exhibit a number of biological and medicinal activities. Many of these compounds are known as antimicrobial [27], insecticidal [28], molluscicidal [29], analgestic [30], anti-inflammatory [31] and anticancer [32]. Furthermore, these compounds act as potential inhibitors of human Chk1 kinase [33]. More recently, a number of dihydropyrano[2,3-c]pyrazoles have been found to be the potential inhibitors of yeast α-glucosidase [34]. One of the most important and convenient procedure for the synthesis of dihydropyrano[2,3-c]pyrazoles is the use of a four-component reaction of aldehyde, ethyl acetoacetate, malononitrile and hydrazine hydrate promoted by some catalysts such as triethylamine [35, 36], piperidine [37], L-proline [38], imidazole [39], per-6-amino-β-cyclodextrin [40], γ-alumina [41], TEAB [42], $H_4[SiW_{12}O_{40}]$ [43], amberlyst A21 [44], basic and acidic ionic liquids [45–47], meglumine [48], cocamidopropyl betaine [49], $Na_2CaP_2O_7$ [50] and lipase enzyme [51]. Although some of these methods have convenient protocols with good to high yields, the majority of these methods are associated with some limitations such as the use of expensive catalyst, using excess amount of hydrazine hydrate, high temperature, long reaction time, high toxicity of the used catalyst and using non reusable catalyst.

Herein we report an efficient and environmentally benign method for the synthesis of dihydropyrano[2,3-c]pyrazoles by using a four-component reaction of aldehyde, ethyl acetoacetate, malononitrile and hydrazine hydrate in the presence of $Ca_{9.5}Mg_{0.5}(PO_4)_{5.5}(SiO_4)_{0.5}F_{1.5}$ (Si–Mg-FA) as a new cooperative catalyst under mild and heterogeneous conditions (Scheme 1).

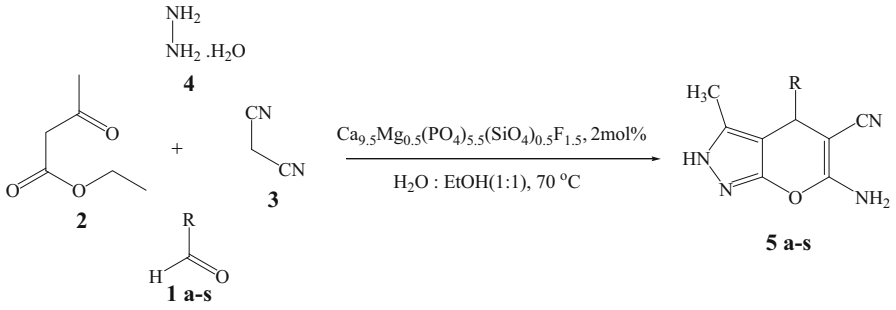

Scheme 1 The synthesis of dihydropyrano[2,3-c]pyrazoles in the presence of $Ca_{9.5}Mg_{0.5}(PO_4)_{5.5}(SiO_4)_{0.5}F_{1.5}$ as a new cooperative catalyst

Experimental

All reagents were purchased from Merck and Aldrich and used without further purification. All yields refer to isolated products after purification. The products were characterized by comparison of physical data with those of known compounds and by spectroscopic data (FTIR, ^{1}HNMR and ^{13}CNMR spectra). ^{1}HNMR spectra were recorded with a Bruker Avance 400 (400 MHz) in DMSO-d_6 as the solvent. Apatite derivatives nanopowders were synthesized according to the previous works [24] by a high energy planetary ball mill (Fretch Pulversette 5) with a 125 mL zirconia vial and four 20 mm diameter zirconia balls at room temperature. The morphology and particle size of the catalyst were measured by using transmission electron microscopy (TEM, Philips CM-FG120) at 200 kV. The BET surface area and pore volume were measured by using a KELVIN sorptometer 1042 with nitrogen adsorption and desorption isotherms at 77 K. All samples were degassed at 100 °C for 130 min. pH of all samples were measured by using a suspension of 1.00 g of milled apatite derivative in 200 mL of distilled water with a magnetic stirrer. Pyridine adsorption was studied by employing 0.2 g of catalyst (pre-activated at 350 °C for 2 h) exposed to dry pyridine vapors in a vacuum desiccator [52]. Phase structure analyses were determined by X-ray diffractometer (XRD, Philips Xpert) using the Ni-filtered Cu K_α ($\lambda_{CuK\alpha} = 0.1542$ nm, radiation at 40 kV and 30 mA). The data were collected over the 2θ range of 10°–70°, time per step was 2.5 s and step size was 0.021°.

Preparation of $Ca_{9.5}Mg_{0.5}(PO_4)_{5.5}(SiO_4)_{0.5}F_{1.5}$

A mixture of calcium hydroxide (2.594 g, 35 mmol), diphosphorous pentoxide (1.562 g, 11 mmol), calcium fluoride (0.234 g, 3 mmol), magnesium hydroxide (0.117 g, 2 mmol) and silicon dioxide (0.120 g, 2 mmol) was mechanochemically activated by using a high energy planetary ball mill (Fretch Pulverisette 5) with a 125 mL zirconia vial and four 20 mm diameter zirconia balls. The rotation speed was 250 rpm and the ball milling process was carried out at ambient temperature for 12 h. The catalyst synthesis reaction is proposed according to the following equation:

$$35Ca(OH)_2 + 11P_2O_5 + 3CaF_2 + 2Mg(OH)_2 + 2SiO_2 \rightarrow 4Ca_{9.5}Mg_{0.5}(PO_4)_{5.5}(SiO_4)_{0.5}F_{1.5} + 37H_2O$$

General procedure for the synthesis of dihydropyrano[2,3-c]pyrazoles

An aldehyde (2 mmol), malononitrile (2 mmol) and $Ca_{9.5}Mg_{0.5}(PO_4)_{5.5}(SiO_4)_{0.5}F_{1.5}$ (0.04 g, 2 mol%) were added to a stirred mixture of ethyl acetoacetate (2 mmol) and hydrazine hydrate (2 mmol) in 8 mL of EtOH/H_2O (1:1). The resulting mixture was heated at 70 °C for the specified time. After the completion of the reaction,

monitored by TLC, ethanol (2 × 20 mL) was added to the reaction mixture and heated to dissolve the product. Then, the reaction mixture was filtered to separate the catalyst. The collected EtOH was evaporated under reduced pressure to give the crude product. The further purification was sought by recrystallization in EtOH/H_2O (9:1).

Results and discussion

As it was cited, the applications of synthetic HA as a catalyst are restricted because of its high solubility, poor mechanical properties and high sensitivity to acidic conditions. Also, the surface area and the porosity of HA are less than those of the common catalysts. These limitations can be decreased by incorporation of an appropriate molar ratio of F, Mg and Si into HA structure. In the previous work, the synthesis and characterization of nanosized silicon and magnesium co-doped fluorapatite ($Ca_{9.5}Mg_{0.5}(PO_4)_{5.5}(SiO_4)_{0.5}F_{1.5}$, Si–Mg-FA) were studied by high energy ball milling [24]. With regard to these molar ratios, this advanced material is formed in biological apatite structure with 24 nm average size [24] (Fig. 1). Moreover, the results of EDX analysis and elemental maps show homogenous distribution of elements in the structure of Si–Mg-FA (Fig. 2). In the present work, the surface area of this material and its catalytic activity were studied for the synthesis of dihydropyrano[2,3-c]pyrazoles by a four-component reaction of aldehyde, ethyl acetoacetate, malononitrile and hydrazine hydrate.

At first, to optimize the reaction conditions, a one-pot reaction of 4-chlorobenzldehye, ethyl acetoacetate, malononitrile and hydrazine hydrate was studied in the presence of the catalytic amount of Si–Mg-FA under different conditions (Table 1). When the reaction was carried out in the absence of the catalyst, the corresponding product was obtained in low yield after prolonged reaction time (Table 1, entry 1). The reaction carried out in absence of solvent gave lower yield comparing to solvent

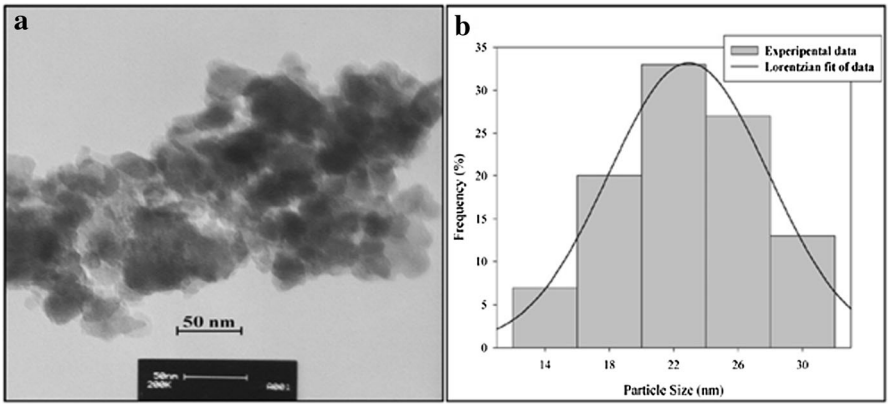

Fig. 1 **a** TEM images of $Ca_{9.5}Mg_{0.5}(PO_4)_{5.5}(SiO_4)_{0.5}F_{1.5}$. **b** Particle size distribution histogram of $Ca_{9.5}Mg_{0.5}(PO_4)_{5.5}(SiO_4)_{0.5}F_{1.5}$

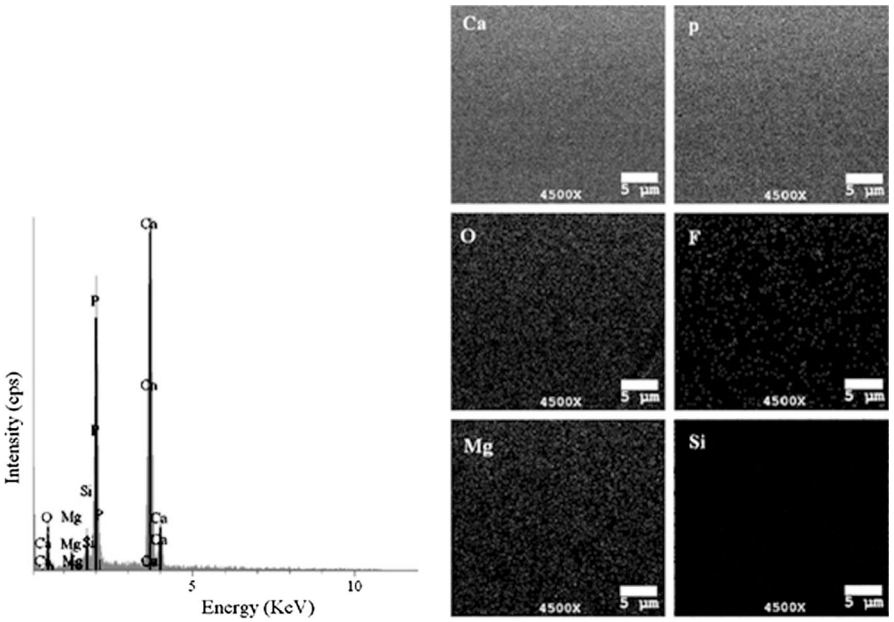

Fig. 2 EDX analysis and elemental mapping of Si–Mg-FA

Table 1 Optimization of the reaction conditions for the synthesis of 6-amino-4-(4-chlorophenyl)-3-methyl-2,4-dihydropyrano[2,3-c]pyrazole-5-carbonitrile

Entry	Solvent	Amount of catalyst (mol%)	Time (min)	Temp. (°C)	Yield (%)[a]
1	H_2O/EtOH (1:1)	–	180	70	35
2	EtOH	2	120	70	66
3	H_2O	2	120	70	50
4	–	2	120	70	20
5	H_2O/EtOH (1:1)	2	120	r.t.	45
6	H_2O/EtOH (1:1)	2	120	50	82
7	H_2O/EtOH (1:1)	1	120	70	78
8	H_2O/EtOH (1:1)	2	60	70	90
9	H_2O/EtOH (1:1)	3	60	70	90

Reaction conditions: 4-chlorobenzaldehyde (2 mmol), ethyl acetoacetate (2 mmol), malononitrile (2 mmol), hydrazine hydrate (2 mmol), solvent [H_2O/EtOH:4 mL/4 mL]

[a] The yields refer to the isolated pure products

mediated reactions. It may be due to the lower homogeneity of the reaction under solvent-free conditions (Table 1, entry 4). The results displayed that the best yield of the product was obtained when the reaction was carried out in H_2O/EtOH (1:1, V/V) at 70 °C by using 2 mol% of the catalyst (Table 1, entry 8). It should be

mentioned that an increase of the amount of the catalyst did not improve the yield of the reaction (Table 1, entry 9).

After optimizing the reaction conditions, to show the generality of the present work, a number of four-component reactions of various aldehydes with ethyl acetoacetate, malononitrile and hydrazine hydrate were studied under the optimized conditions (Table 2). Using the present cooperative catalyst, a variety of aromatic and heteroaromatic aldehydes were easily converted to their corresponding dihydropyrano[2,3-c]pyrazole derivatives in good to high yields. Aromatic aldehydes with different functional groups were subjected to the condensation reaction and the resulting products were synthesized in good to high yields and relatively short reaction time. It should be mentioned that the steric effects of ortho substitutions on the aromatic aldehydes not only decreased the reaction yields but also increased the reaction time (Table 2, entries 2, 3, 7). It was notable that the methoxycarbonyl group on the aromatic aldehyde was intact during the course of the reaction (Table 2, entry 12). It may be due to employing mild reaction conditions and

Table 2 The synthesis of dihydropyrano[2,3-c]pyrazoles from various aromatic aldehydes, malononitrile, ethyl acetoacetate and hydrazine hydrate catalyzed by $Ca_{9.5}Mg_{0.5}(PO_4)_{5.5}(SiO_4)_{0.5}F_{1.5}$

Entry	Aldehyde	Product	Time (min)	Yield (%)[a]	M.P. (°C) found	M.P (°C) reported
1	4-Cl–C_6H_4–CHO	4 a	60	90	236–237	234–235 [48]
2	2-Cl–C_6H_4–CHO	4 b	120	76	246–247	245–246 [48]
3	2,6-$(Cl)_2$–C_6H_3–CHO	4 c	150	73	246–248	249–250 [36]
4	4-F–C_6H_4–CHO	4 d	75	88	243–245	244–245 [48]
5	4-Br–C_6H_4–CHO	4 e	90	83	180–181	178–180 [41]
6	C_6H_5–CHO	4 f	90	81	242–244	243–244 [48]
7	2-NO_2–C_6H_4–CHO	4 g	120	79	242–243	243–244 [48]
8	3-NO_2–C_6H_4–CHO	4 h	60	82	234–236	232–234 [45]
9	4-NO_2–C_6H_4–CHO	4 i	70	88	245–247	248–249 [48]
10	4-CH_3O–C_6H_4–CHO	4 j	40	87	211–213	210–212 [48]
11	3,4-$(CH_3O)_2$–C_6H_3–CHO	4 k	60	78	194–195	192–194 [41]
12	4-CH_3OOC–C_6H_4–CHO	4 l	60	74	242–244	240–242 [36]
13	3-HO–C_6H_4–CHO	4 m	120	76	222–224	220–222 [51]
14	4-CN–C_6H_4–CHO	4 n	75	84	215–216	212–214 [47]
15	2-Furyl–CHO	4 o	70	81	234–236	232–234 [45]
16	2-Thienyl–CHO	4 p	70	83	223–225	224–226 [48]
17	3-Pyridyl–CHO	4 q	90	84	216–218	215–216 [51]
18	$CH_3(CH_2)_4$–CHO	4 r	150	–	–	–
19	$CH_3(CH_2)_2$–CHO	4 s	150	–	–	–

The reaction was carried out at 70 °C by using aldehyde (2 mmol), ethyl acetoacetate (2 mmol), malononitrile (2 mmol), hydrazine hydrate (2 mmol) and 2 mol% of the catalyst in 8 mL of H_2O/EtOH (1:1)

[a] The yields refer to the isolated pure products

catalyst. Heterocyclic aldehydes such as furan-2-carbaldehyde, thiophen-2-carbaldehyde and 3-pyridine carbaldehyde were converted to the corresponding products in good yields (Table 2, entries 15–17). It should be declared that the present procedure was not suitable for the conversion of aliphatic aldehydes to the corresponding dihydropyrano[2,3-c]pyrazole derivatives (Table 2, entries 18–19).

Based on the obtained results and the literature survey, we suggest a mechanism for these reactions by using catalytic amount of Si–Mg-FA (Scheme 2). First, pyrazolone (I) is easily formed by the condensation of hydrazine and ethyl acetoacetate. Then fluoride ion in Si–Mg-FA catalyzes the Knoevenagel condensation of malononitrile and an aldehyde (activated by Mg^{2+} of the catalyst) to form arylidenemalononitrile as the intermediate (II). Next, the Michael addition of

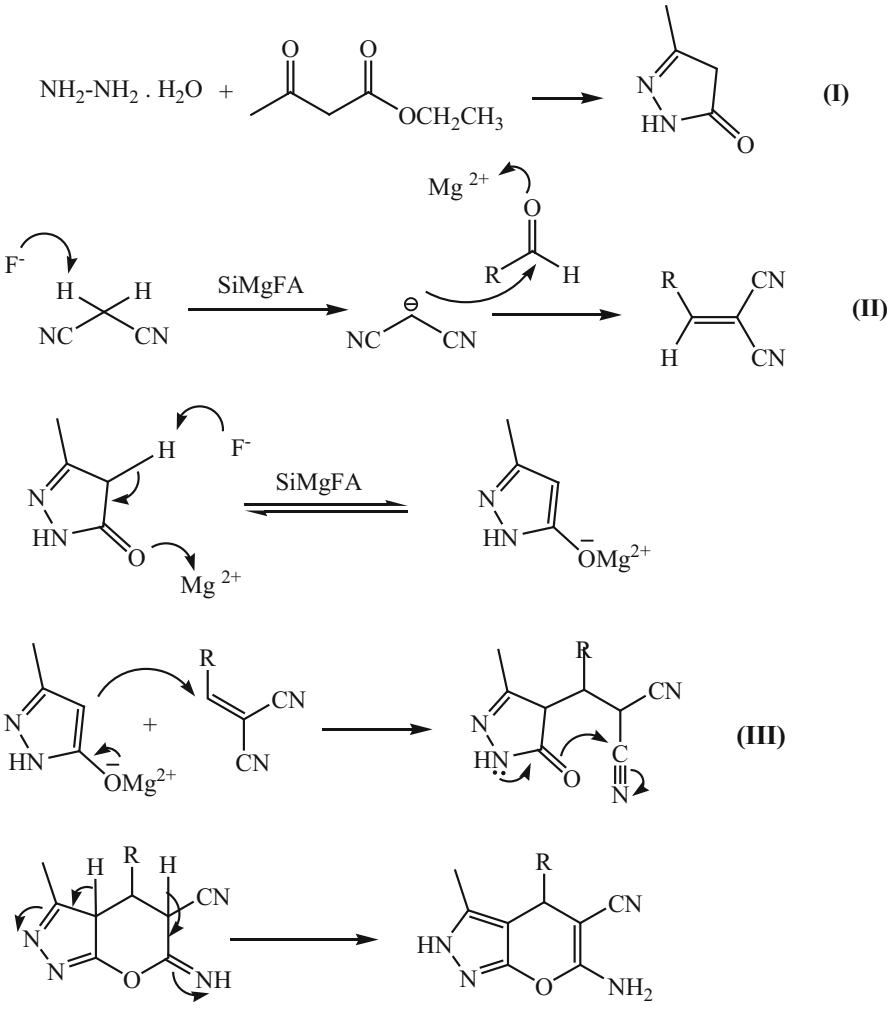

Scheme 2 Suggested mechanism for the synthesis of dihydropyrano[2,3-c]pyrazoles using Si–Mg-FA

enolized pyrazolone (promoted by Mg^{2+} and F^- of the catalyst) to arylidene-malononitrile is carried out to produce the intermediate (III). Finally, the corresponding product is formed by intramolecular cyclization and tautomerization of the intermediate (III).

As shown in Scheme 2, in the structure of the catalyst, F^- can be used as a Brønsted base and Mg^{2+} as a Lewis acid. Mg^{2+} as a hard acid can be coordinated by oxygen lone pair electrons of aldehyde or pyrazolone as the hard bases [53]. We think that these hard–hard O:Mg^{2+} interactions can increase the rate and the yield of the reaction. To study this hypothesis, the reaction of 4-chlorobenzaldehyde, ethyl acetatoacetate, malononitrile and hydrazine hydrate was studied in the presence of various apatites under the same conditions (Table 3). The apatite derivatives used as the catalysts were synthesized by high energy ball milling technique according to the previous works [13, 24]. It should be mentioned that the effect of some parameters such as specific surface area, pore volume, particle size, pH and crystallinity degree of these apatites was studied on the yield and reaction time. As already mentioned, the synthesis of dihydropyrano[2,3-c]pyrazoles using a four-component reaction of an aldehyde, ethyl acetatoacetate, malononitrile and hydrazine hydrate is commonly catalyzed by basic catalysts. Therefore, the basic strength of the catalyst can be an important factor to increase the reaction rate. Among the present apatite derivatives, HA has the highest basicity. However, Si–Mg-FA with the lowest basicity produced the maximum yield in the shortest reaction time (Table 3, entry 4). We also studied the surface area (S_{BET}) and pore volume (V_{pore}) of these apatites. The findings demonstrated that by incorporation of magnesium and silicon into the structure of apatite, the surface area and pore volume of the catalyst increased (Table 3). By comparison of the obtained results, it was found that the effect of silicon on the surface parameters was more than that of magnesium. It is known that by improving the surface factors, the efficiency of the catalyst increases. Although Si–Mg-FA has the highest surface area and pore volume among these apatite derivatives, we think that they cannot be the sufficient reasons for the most increase of the reaction rate and yield. Another parameter studied was the particle sizes of the present catalysts. Because the particle sizes of these apatite derivatives are almost the same. It seems that this factor cannot obviously affect the reaction rate (Table 3).

It seems that Mg^{2+} in the structure of Si–Mg-FA can act as a Lewis acid and can be coordinated by oxygen lone pair electrons of aldehydes to promote the Knoevenagel reaction rate. Furthermore, the dehydration process of the Knoevenagel condensation can also be accelerated by magnesium cation. As it was cited in the suggested mechanism, the enolization of pyrazolone can be promoted by Mg^{2+} of the catalyst [54]. To exhibit the Lewis acid sites of Mg^{2+} in the structure of the catalyst, the FT-IR spectroscopy of pyridine adsorption technique was used at different temperature. Before studying this technique, it should be stated that in the FT-IR spectroscopy of FA, Mg-FA and Si–Mg-FA, a broad peak around 3400 cm^{-1} is corresponding to the stretching vibrations of hydroxyl groups of adsorbed water. A peak at 1640 cm^{-1} indicates the bending vibrations of hydroxyl groups of adsorbed water. The appearance of a doublet peak at 1425 and 1474 cm^{-1} is

Table 3 Synthesis of 6-amino-4-(4-chlorophenyl)-3-methyl-2,4-dihydropyrano[2,3-c]pyrazole-5-carbonitrile catalyzed by apatite derivatives

Entry	Apatite	Particle size (nm)	S_{BET} (m^2/g)	V_{Pore} (cm^3/g)	PH	Crystallinity degree (%)	Time (min)	Yield (%)[a]
1	$Ca_{10}(PO_4)_6(OH)_2$	20–40	8.105	1.846	11.6	72	75	86
2	$Ca_{10}(PO_4)_6(F)_2$	35–70	13.864	3.158	11.2	56	120	81
3	$Ca_{9.5}Mg_{0.5}(PO_4)_6(F)_2$	30–100	16.059	3.658	10.9	47	120	79
4	$Ca_{9.5}Mg_{0.5}(PO_4)_{5.5}(SiO_4)_{0.5}F_{1.5}$	20–30	23.535	5.361	9.9	39	60	90

The reaction was performed by using 4-chlorobenzaldehyde (2 mmol), ethyl acetoacetate (2 mmol), malononitrile (2 mmol) and hydrazine hydrate (2 mmol) in the presence of 2 mol% of the catalyst

All reactions were carried out at 70 °C in 8 mL of H_2O/EtOH (1:1)

[a] The yields refer to the isolated pure products

attributed to symmetric and asymmetric stretching vibrations of the trace amount of CO_3^{2-} (Fig. 3) [24]. The stretching vibrations of PO_4^{3-} are located in the range of 1000–1300 cm^{-1}. A doublet peak located at 574 and 603 cm^{-1} is attributed to symmetric and asymmetric bending vibrations of PO_4^{3-} [24]. In Si–Mg-FA, the stretching vibrations of SiO_4^{4-} are overlapped by the stretching vibrations of PO_4^{3-} [24].

The spectrum of pyridine adsorbed Si–Mg-FA at room temperature shows a peak at 1457 cm^{-1}, which is characteristic for Lewis acid sites (Fig. 4) [52]. It should be mentioned that this peak overlaps with the bands of carbonate ion. The absence of the bands at 1540 and 1640 cm^{-1} demonstrates that there is no Brønsted acid site in this material [52]. After heating the catalyst at 50 °C, pyridine was obviously desorbed from the Lewis acid sites indicated by the decrease in intensity of the corresponding peak. As shown in Fig. 4, pyridine was completely desorbed by further heating at 100 °C. These results confirm the presence of Lewis acid sites in the structure of this nano catalyst attributed to magnesium cations. The decrease in the intensity of the band at 50 °C and its disappearance at 100 °C demonstrate a weak interaction of pyridine with Si–Mg-FA. This is justifiable because Mg^{2+} is not introduced as a strong Lewis acid [53].

To extend this scope, we also studied the FT-IR spectroscopy of pyridine adsorption of Mg-FA ($Ca_{9.5}Mg_{0.5}(PO_4)_6(F)_2$). At first, the FT-IR spectroscopy of Mg-FA was studied and the presence of a weak peak around 1432 cm^{-1} was attributed to the trace amount of CO_3^{2-} (Fig. 5). Although there are magnesium cations in the structure of Mg-FA, the spectrum of pyridine adsorbed Mg-FA at room temperature shows no peak around 1455 cm^{-1} to exhibit the existence of Lewis acid sites in the structure of $Ca_{9.5}Mg_{0.5}(PO_4)_6(F)_2$.

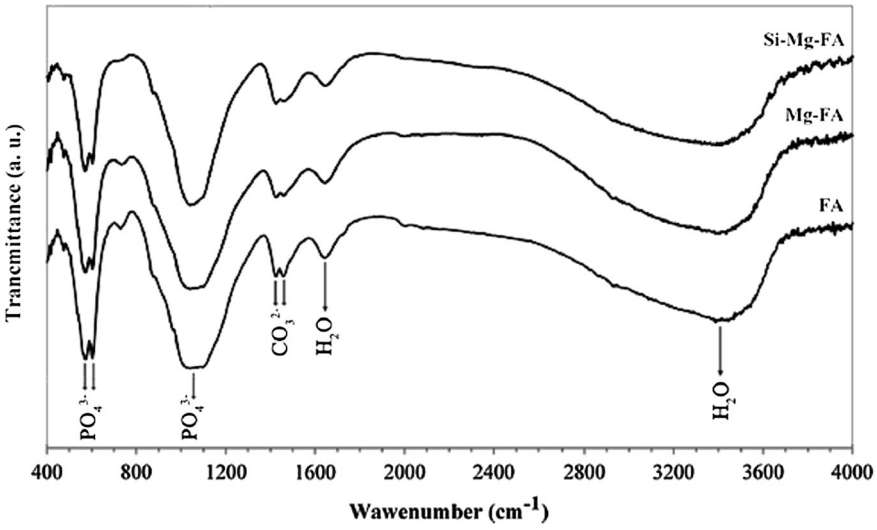

Fig. 3 FT-IR spectra of FA, Mg-FA and Si–Mg-FA

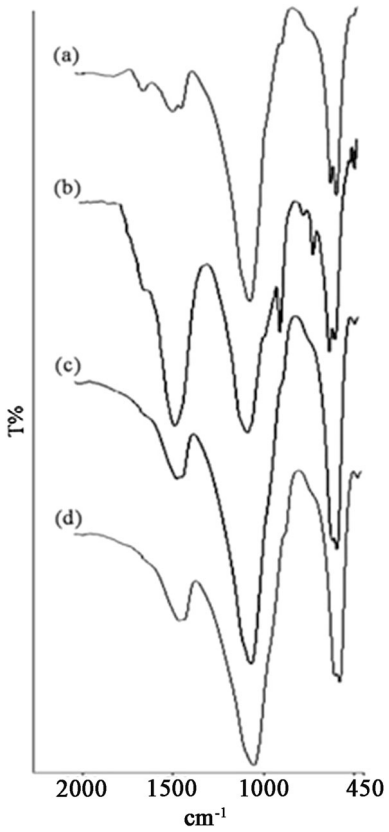

Fig. 4 **a** FT-IR spectrum of Si–Mg-FA. **b** FT-IR spectrum of Si–Mg-FA after pyridine adsorption at room temperature. **c** FT-IR spectrum of pyridine retention on Si–Mg-FA at 50 °C. **d** FT-IR spectrum of pyridine retention on Si–Mg-FA at 100 °C

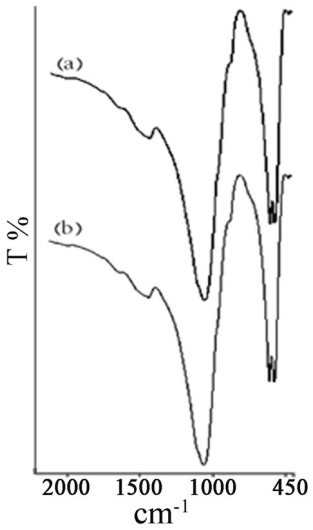

Fig. 5 **a** FT-IR spectrum of Mg-FA. **b** FT-IR spectrum of Mg-FA after pyridine adsorption at room temperature

It seems that the crystallinity degree of these materials may act as the key role for these observations. It is well known that crystallinity refers to the degree of structural order in a solid. In a crystal, the atoms or molecules are arranged in a regular and periodic manner. Moreover, the degree of crystallinity has a big influence on hardness, density, transparency and diffusion. Many materials such as ceramics can be prepared in such a way as to produce a mixture of crystalline and amorphous regions. In such cases, crystallinity is usually specified as a percentage of the volume of the material that is crystalline. It is known that the apatite derivatives crystallize in the hexagonal crystal system so that most of cations (e.g. Ca^{2+} or Mg^{2+}) are placed into the lattice and the exchangeable anions (e.g. OH^- or F^-) are located at the edges [24]. In the present work, the crystallinity degree of HA, FA, Mg-FA and Si–Mg-FA was obtained from their XRD patterns according to the previous works [13, 24]. It should be cited that the crystallinity degree of samples (*Xc*) corresponding to the fraction of crystalline phase present in the examined volume was evaluated by the following equation [24]: $Xc = 1 - (V_{112/300}/I_{300})$, where I_{300} is the intensity of (300) reflection, and $V_{112/300}$ is the intensity of the hollow volume between (112) and (300) reflections (Fig. 6).

As shown in Table 3, among these apatite derivatives, HA has the most crystallinity degree value (72%) and Si–Mg-FA has the least one (39%). The decrease of the crystallinity degree of Si–Mg-FA is due to the change of the lattice parameters formed by simultaneous incorporation of F, Mg and Si into the lattice of apatite [24]. Because the ionic radii of Mg^{2+}, F^- and SiO_4^{4-} are different from those of Ca^{2+}, OH^- and PO_4^{3-}, the partial substitution of Ca^{2+} by Mg^{2+}, the substitution of F^- instead of OH^- and the partial substitution of PO_4^{3-} by SiO_4^{4-} change the lattice parameters of the primitive apatite [24]. We think that by decreasing the crystallinity degree of these apatite derivatives, the availability to the cations placed into the lattice becomes easier. This is agreeable with the results of FT-IR spectra of pyridine adsorbed Mg-FA and Si–Mg-FA. Although both

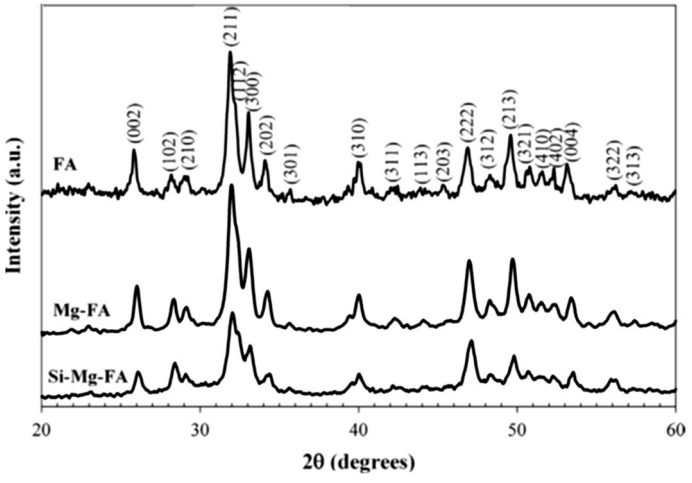

Fig. 6 XRD patterns of FA, Mg–FA and Si–Mg–FA

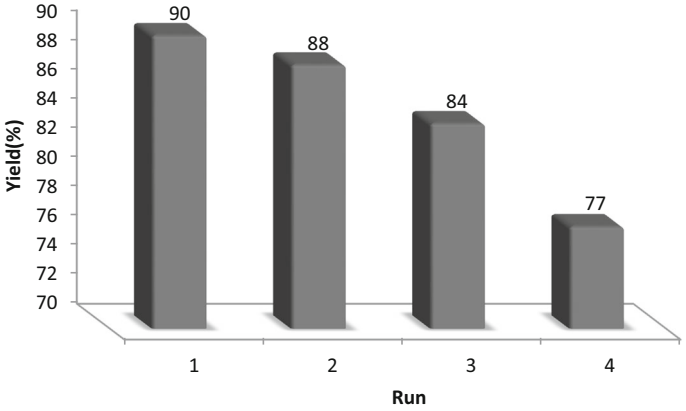

Fig. 7 Reusability of the catalyst for the synthesis of 6-amino-4-(4-chlorophenyl)-3-methyl-2,4-dihydropyrano[2,3-c]pyrazole-5-carbonitrile. The reaction was carried out with 4-chlorobenzaldehyde (2 mmol), ethyl acetoacetate (2 mmol), malononitrile (2 mmol), hydrazine hydrate (2 mmol) and reused catalyst (2 mol%) in 8 mL of H_2O/EtOH (1:1) at 70 °C for 60 min

$Ca_{9.5}Mg_{0.5}(PO_4)_6(F)_2$ and $Ca_{9.5}Mg_{0.5}(PO_4)_{5.5}(SiO_4)_{0.5}F_{1.5}$ have 0.5 mol of magnesium in their structures, the interaction between Mg^{2+} and pyridine was only observed for Si–Mg-FA. Because the crystallinity degree of Si–Mg-FA is lower than that of Mg-FA, magnesium cations in the structure of $Ca_{9.5}Mg_{0.5}(PO_4)_{5.5}(SiO_4)_{0.5}F_{1.5}$ are more available than those of $Ca_{9.5}Mg_{0.5}(PO_4)_6(F)_2$. It is noteworthy that by the incorporation of Si to the structure of Mg-FA, the surface area increases and the crystallinity degree value decreases which these factors lead to increase the availability to magnesium cations. Therefore, Si–Mg-FA not only can be introduced as a Brønsted basic catalyst but also can act as a Lewis acid catalyst. Consequently, Si–Mg-FA can be introduced as a cooperative catalyst. This may be the logical reason why Si–Mg-FA is the best catalyst among the present apatite derivatives for the synthesis of dihydropyrano[2,3-c]pyrazoles.

The reusability of the catalyst was studied for the reaction of 4-chlorobenzldehye, ethyl acetoacetate, malononitrile and hydrazine hydrate under optimized conditions. For this purpose, after the completion of each reaction, the hot ethanol was added to the reaction mixture to dissolve the product. After that, the catalyst was separated by filtration and dried in an oven at 120 °C for 2 h to use for the next reaction. The findings showed that the catalyst could be used four times with losing its activity gradually. As shown in Fig. 7, the product of 6-amino-4-(4-chlorophenyl)-3-methyl-2,4-dihydropyrano[2,3-c]pyrazole-5-carbonitrile was obtained in 77% yield by using 2 mol% of the reused catalyst in the fourth time use. It should be noted that the reusability study of the present catalyst was followed by increasing the amount of the reused catalyst under optimized conditions. The experimental results exhibited that the corresponding product was obtained in 79% yield by using 3 mol% of the reused catalyst in the fourth time use. These findings displayed that a significant improvement was not observed in the product yield by an increase of the reused catalyst to 3 mol%.

Table 4 Comparison of Si–Mg-FA with different catalysts for the synthesis of 6-amino-4-(4-chlorophenyl)-3-methyl-2,4-dihydropyrano[2,3-c]pyrazole-5-carbonitrile

Entry	Catalyst	Conditions	Time (min)	Yield (%)	Ref.
1	δ-Alumina (30 mol%)	H_2O, reflux	35	90	41
2	$Na_2CaP_2O_7$ (20 mol%)	H_2O, reflux	15	86	50
3	Imidazole (50 mol%)	H_2O, 80 °C	20	90	39
4	Amberlyst A21 (30 mg)	EtOH, r.t.	15	98	44
5	L-proline (10 mol%)	H_2O, reflux	10	94	38
6	[Hmim]HSO_4 (10 mol%)	Ethanol 50%, 50 °C	25	92	47
7	Meglumine (10 mol%)	EtOH:H_2O (9:1), r.t.	15	90	48
8	KF/Al_2O_3 (30 mol%)	H_2O, reflux	35	88	41
9	Si–Mg-FA (2 mol %)	H_2O:EtOH (1:1), 70 °C	60	90	This work

Finally, to show the merit of this method, the efficacy of the present catalyst was compared with some reported catalysts for the synthesis of 6-amino-4-(4-chlorophenyl)-3-methyl-2,4-dihydropyrano[2,3-c]pyrazole-5-carbonitrile. As shown in Table 4, Si–Mg–FA is comparable with the most of the reported catalysts in viewpoints of yield and reaction time. Moreover, the present catalyst is superior in terms of using low amount of the catalyst. The use of green and reusable catalyst, non-toxic solvent, mild reaction conditions and simple procedure are the other advantages of the present work.

Conclusion

In summary, we introduced $Ca_{9.5}Mg_{0.5}(PO_4)_{5.5}(SiO_4)_{0.5}F_{1.5}$ as a nano cooperative catalyst to promote the one-pot synthesis of dihydropyrano[2,3-c]pyrazoles. The reactions were carried out in aqueous ethanol under mild conditions. The catalytic activity of this catalyst was compared with those of the other hydroxyapatite derivatives in the synthesis of dihydropyrano[2,3-c]pyrazoles. The existence of Brønsted base and Lewis acid sites in the structure of $Ca_{9.5}Mg_{0.5}(PO_4)_{5.5}(SiO_4)_{0.5}F_{1.5}$ made it the best catalyst among the other hydroxyapatite derivatives. Using a cooperative catalyst and an environmentally benign procedure with good to high yield of the products were the other advantages of the present method.

Acknowledgements We gratefully acknowledge the funding support received for this project from the Islamic Azad University, Khorasgan and fasa Branches.

References

1. Li M, Fang Z, Smith RL, Yang S (2016) Prog Energy Combust Sci 55:98–194
2. Peters R (2015) Cooperative catalysis. Wiley, Weinheim
3. Descamps M, Hornez JC, Leriche A (2009) J Eur Ceram Soc 29:369–375
4. Mazaheri M, Haghighatzadeh M, Zahedi AM, Sadrnezhaad SK (2009) J Alloys Compd 471:180–184

5. Arami H, Mohajerani M, Mazloumi M, Khalifehzadeh R, Lak A, Sadrnezhaad SK (2009) J Alloys Compd 469:391–394
6. Wang J, Chao Y, Wan Q, Zhu Z, Yu H (2009) Acta Biomater 5:1798–1807
7. Mostafa NY, Hassan HM, Mohamed FH (2009) J Alloys Compd 479:692–698
8. Chen Y, Miao X (2004) Ceram Int 30:1961–1965
9. Basar B, Tezcaner A, Keskin D, Evis Z (2010) Ceram Int 36:1633–1643
10. Turkoza M, Atillab AO, Evisc Z (2013) Ceram Int 39:8925–8931
11. Chen Y, Miao X (2005) Biomaterials 26:1205–1210
12. Eslami H, Solati-Hashjin M, Tahriri M (2009) Mater Sci Eng C 29:1387–1398
13. Fathi MH, Mohammadi Zahrani E (2009) J Cryst Growth 311:1392–1403
14. Suchanek WL, Byrappa K, Shuk P, Riman RE, Janas VF, TenHuisen KS (2004) Biomaterials 25:4647–4657
15. Mroz W, Bombalska A, Burdynska S, Jedynski M, Prokopiuk A, Budner B, Slosarczyk A, Zima A, Menaszek E, Scisłowska-Czarnecka A, Niedzielski K (2010) J Mol Struct 977:145–152
16. Webster TJ, Ergun C, Doremus RH, Bizios R (2002) J Biomed Mater Res 59:312–317
17. Sun ZP, Ercan B, Evis Z, Webster TJ (2010) J Biomed Mater Res 94A:806–815
18. Kheradmandfard M, Fathi MH (2010) J Alloys Compd 504:141–145
19. Cai Y, Zhang S, Zeng X, Wang Y, Qian M, Weng W (2009) Thin Solid Films 517:5347–5351
20. Portera AE, Patela N, Skepper JN, Best SM, Bonfield W (2003) Biomaterials 24:4609–4620
21. Balamurugan A, Rebelo AHS, Lemos AF, Rocha JHG, Ventura JMG, Ferreira JMF (2008) Dent Mater 24:1374–1380
22. Hijon N, Cabanas MV, Pena J, Vallet-Regi M (2006) Acta Biomater 2:567–574
23. Aminian A, Solati-Hashjin M, Samadikuchaksaraei A, Bakhshi F, Gorjipour F, Farzadi A, Moztarzadeh F, Schmucker M (2011) Ceram Int 37:1219–1229
24. Ahmadia T, Monshi A, Mortazavi V, Fathi MH, Sharifi S, HashemiBeni B, MoghareAbed A, Kheradmandfard M, Sharifnabi A (2014) Ceram Int 40:8341–8349
25. Ragel CV, Vallet-Regí M, Rodríguez-Lorenzo LM (2002) Biomaterials 23:1865–1872
26. Fathi MH, Zahrani EM (2008) Iran J Pharm Res 4:209–213
27. El-Tamany ES, El-Shahed FA, Mohamed BH (1999) J Serb Chem Soc 64:9–18
28. Ismail ZH, Aly GM, El-Degwi MS, Heiba HI, Ghorab MM (2003) Egypt J Biotechnol 13:73–82
29. Abdelrazak FM, Metz P, Kataeva O, Jager A, El-Mahrouky SF (2007) Arch Pharm Chem Life Sci 340:543–548
30. Kuo SC, Huang LJ, Nakamura H (1984) J Med Chem 27:539–544
31. Zaki MEA, Soliman HA, Hiekal OA, Rashad AEZ (2006) Naturoforsch C61:1–6
32. Wang JL, Liu D, Zheng ZJ, Shan S, Han X, Srinivasula SM, Croce CM, Alnemri ES, Huang Z (2007) Proc Natl Acad Sci USA 97:7124–7129
33. Foloppe N, Fisher LM, Howes R, Potter A, Robertos AGS, Surgenor AE (2006) Bioorg Med Chem 14:4792–4802
34. Kashtoh H, Muhammad MT, Khan JJA, Rasheed S, Khan A, Perveen S, Javaid K, Wahab AT, Khan KM, Choudhary MI (2016) Bioorg Chem 65:61–72
35. Litvinov YM, Shestopalov AA, Rodinovskaya LA, Shestopalov AM (2009) J Comb Chem 11:914–919
36. Litvinov YM, Rodinovskaya LA, Shestopalov AM (2009) Russ Chem Bull Int Ed 58:2362–2368
37. Vasuki G, Kumaravel K (2008) Tetrahedron Lett 49:5636–5638
38. Mecadon H, Rohman MR, Kharbangar I, Laloo BM, Kharkongor I, Rajbangshi M, Myrboh B (2011) Tetrahedron Lett 52:3228–3231
39. Siddekha A, Nizam A, Pasha MA (2011) Spectrochim Acta A 81:431–440
40. Kanagaraj K, Pitchumani K (2010) Tetrahedron Lett 51:3312–3316
41. Mecadon H, Rohman MR, Rajbangshi M, Myrboh B (2011) Tetrahedron Lett 52:2523–2525
42. Kumar GS, Kurumurthy C, Veeraswamy B, Rao PS, Narsaiah B (2013) Organic Prep Proc Int 45:429–436
43. Chavan HV, Babar SB, Hoval RU, Bandgar BP (2011) Bull Korean Chem Soc 32:3963–3966
44. Bihani M, Bora PP, Bez G, Askari H (2013) Sustain Chem Eng 1:440–447
45. Khurana JM, Chaudhary A (2012) Green Chem Lett Rev 5:633–638
46. Ebrahimi J, Mohanndi A, Pakjoo V, Bahramzadeh E, Habibi A (2012) J Chem Sci 124:1013–1017
47. Khazdooz L, Zarei A (2016) Iran J Catal 6:69–74
48. Guo RY, An ZM, Mo LP, Yang ST, Liu HX, Wang SX, Zhang ZH (2013) Tetrahedron 69:9931–9938

49. Tamaddon F, Alizadeh M (2014) Tetrahedron Lett 55:3588–3591
50. Maleki B, Nasiri N, Tayebee R, Khojastehnezhad A, Akhlaghi HA (2016) RSC Adv 6:79128–79134
51. Bora PP, Bihani M, Bez G (2013) J Mol Catal B 92:24–33
52. Tyagi B, Chudasama CD, Jasra RV (2006) Appl Clay Sci 31:16–28
53. Ho TL (1977) Hard and soft acid and bases principle in organic chemistry. Academic Press, New York
54. Carey FA, Sundberg RJ (1990) Advanced organic chemistry, part B: reactions and synthesis, 3rd edn. Plenum Press, New York and London